Photoinduced Electron Transfer in the Zn-Substituted Cytochrome *c* $Ru(NH_3)_5$(His-33) Derivative Studied by Phosphorescence and Optically Detected Magnetic Resonance Spectroscopy

Li-Hsin Zang and August H. Maki*

Contribution from the Department of Chemistry, University of California, Davis, California 95616. *Received September 13, 1989*

Abstract: The temperature dependence of long-range quenching of the photoexcited triplet state of Zn-substituted cytochrome *c* by $Ru^{III}(NH_3)_5$ covalently attached to histidine-33 has been studied by monitoring the phosphorescence decay kinetics of the electron donor ^{3}ZnP*. A temperature-independent triplet quenching process, possibly due to electron transfer facilitated by nuclear tunneling, is observed between ca. 10 and 100 K with a rate constant of $3.6 \pm 0.2\ s^{-1}$. Other possibilities for the quenching in this range are energy transfer to an as yet unidentified acceptor state of the Ru^{III} complex or magnetic dipole induced quenching by the paramagnetic Ru^{III} complex. Thermally activated quenching, which is attributed to electron transfer, occurs above 100 K. Two regions of Arrhenius-like behavior are observed with a transition at ca. 150 K from $E_a = 1.6$ kcal/mol to $E_a = 5.6$ kcal/mol. It is suggested that this type of non-Arrhenius behavior is the result of "conformational gating" of electron transfer in proteins. Optical detection of triplet-state magnetic resonance measurements were made at 1.2 K on ^{3}ZnP* in Zn-substituted cytochrome *c* and its Ru^{II} and Ru^{III} derivatives. At this temperature the individual sublevel properties are exhibited, rather than their average. Comparison of the individual triplet sublevel decay lifetimes exhibited by the three proteins allows, in principle, the determination of electron spin orientation selectivity in the quenching process. Our data suggest with reasonable confidence that the T_z sublevel, which has its spin angular momentum aligned in the porphyrin plane, exhibits an enhanced quenching probability by Ru^{III}; i.e., its measured quenching rate constant of $5.2 \pm 1.4\ s^{-1}$ exceeds the average quenching constant, $3.6\ s^{-1}$. This suggestion should be treated with some caution, however, because of the relatively large estimated error in the T_z sublevel quenching constant. The errors are larger for the individual T_y and T_x sublevel quenching constants; little can be concluded about their magnitudes from this work. The zero-field splittings are found to be the same within experimental error for the three proteins, but the line widths of the Ru^{III} derivative are significantly broader, suggesting that a local disordering of the protein environment may accompany quenching of ^{3}ZnP* by Ru^{III} in an electron-transfer mechanism.

It is known that electron transfer can take place over long distances through protein interiors. Factors that generally control the electron-transfer rate include the donor–acceptor separation, the thermodynamic driving force, the nature of the intervening medium, and the relative orientations of donor and acceptor moieties. A great deal of experimental research has focused on elucidation of these factors with the use of modified proteins and protein complexes in which redox centers are held at fixed distances and orientations.[1-18] The triplet excited state of Zn porphyrin, ^{3}ZnP*, is a particularly potent electron donor (and acceptor), and for this reason Zn has been introduced into several hemoproteins for the study of photoinduced electron transfer.[8-18] Although many theoretical models have been developed that address the temperature dependence of the electron-transfer process,[19-21] relatively few experiments have been carried out to study the detailed temperature dependence over a wide range; the most detailed measurements have been carried out on bacterial photosynthetic reaction centers by Clayton, Chance, McElroy, and others.[22]

In this paper, we report our measurements of temperature-dependent quenching of ^{3}ZnP* in Zn/Ru-modified horse heart cytochrome *c* (Zn–cyto c/a_5Ru) using phosphorescence and optical detection of triplet-state magnetic resonance (ODMR) spectroscopy. In this derivative, the Fe^{II} of the heme is replaced with Zn^{II}, while pentammineruthenium (a_5Ru) is covalently bound to the surface histidine-33. Thus the donor and acceptor are held at a relatively fixed distance and orientation by the integral protein structure. The decay kinetics of photoexcited Zn–cyto c/a_5Ru have been measured recently at ambient temperatures with transient absorption spectroscopy;[18] ^{3}ZnP* was found to act as an electron donor to Ru^{III} and as an electron acceptor from Ru^{II}. We have used slow-passage ODMR in the liquid He cryogenic region to measure the zero-field splittings of ^{3}ZnP* in the three proteins, Zn–cyto *c*, Zn–cyto c/a_5Ru^{II}, and Zn–cyto c/a_5Ru^{III}. Although the ZFS were found to be identical for each sample, confirming the weakness of the interaction between Ru and ZnP, the ODMR line widths were significantly larger in Zn–cyto c/a_5Ru^{III} than in the two other proteins, the result of greater heterogeneity of the ^{3}ZnP* environment. In our work, the ex-

(1) Nocera, D. G.; Winkler, J. R.; Yocom, K. M.; Bordignon, E.; Gray, H. B. *J. Am. Chem. Soc.* **1984**, *106*, 5145.
(2) McLendon, G. L.; Miller, J. R. *J. Am. Chem. Soc.* **1985**, *107*, 739.
(3) Crutchley, R. J.; Ellis, W. R.; Gray, H. B. *J. Am. Chem. Soc.* **1985**, *107*, 5002.
(4) Bechtold, R.; Kuehn, C.; Lepre, C.; Isied, S. S. *Nature (London)* **1986**, *322*, 286.
(5) Lieber, C. M.; Karas, J. L.; Gray, H. B. *J. Am. Chem. Soc.* **1987**, *109*, 3778.
(6) Hoffman, B. M.; Ratner, M. A. *J. Am. Chem. Soc.* **1987**, *109*, 6237.
(7) McLendon, G.; Pardue, K.; Bak, P. *J. Am. Chem. Soc.* **1987**, *109*, 7450.
(8) McGourty, J. L.; Blough, N. V.; Hoffman, B. M. *J. Am. Chem. Soc.* **1983**, *105*, 4470.
(9) Peterson-Kennedy, S. E.; McGourty, J. L.; Hoffman, B. M. *J. Am. Chem. Soc.* **1984**, *106*, 5010.
(10) Simolo, K. P.; McLendon, G. L.; Mauk, M. R.; Mauk, A. G. *J. Am. Chem. Soc.* **1984**, *106*, 5012.
(11) Ho, P. S.; Sutoris, C.; Liang, N.; Margoliash, E.; Hoffman, B. M. *J. Am. Chem. Soc.* **1985**, *107*, 1070.
(12) McLendon, G.; Winkler, J. R.; Nocera, D. G.; Mauk, M. R.; Mauk, A. G.; Gray, H. B. *J. Am. Chem. Soc.* **1985**, *107*, 739.
(13) Liang, N.; Kang, G. H.; Ho, P. S.; Margoliash, E.; Hoffman, B. M. *J. Am. Chem. Soc.* **1986**, *108*, 4665.
(14) Conklin, K. T.; McLendon, G. *Inorg. Chem.* **1986**, *25*, 4806.
(15) Liang, N.; Pielak, G. J.; Mauk, A. G.; Smith, M.; Hoffman, B. M. *Proc. Natl. Acad. Sci. U.S.A.* **1987**, *84*, 1249.
(16) Gingrich, D. J.; Nocek, J. M.; Natan, M. J.; Hoffman, B. M. *J. Am. Chem. Soc.* **1987**, *109*, 7533.
(17) Axup, A. W.; Albin, M.; Mayo, S. L.; Crutchley, R. J.; Gray, H. B. *J. Am. Chem. Soc.* **1988**, *110*, 435.
(18) Elias, H.; Chou, M. H.; Winkler, J. R. *J. Am. Chem. Soc.* **1988**, *110*, 429.
(19) DeVault, D. *Q. Rev. Biophys.* **1984**, *13*, 387.
(20) Marcus, R. A.; Sutin, N. *Biochim. Biophys. Acta* **1985**, *811*, 265.
(21) Brunschwig, B. S.; Sutin, N. *Comments Inorg. Chem.* **1987**, *6*, 209.
(22) This work is reviewed thoroughly in ref 19.

0002-7863/90/1512-4346$02.50/0

cited-state decay kinetics were inferred from the phosphorescence decay of ^{3}ZnP*, which was observed between ca. 10 and 200 K. Of particular interest was the observation of a weak, temperature-independent quenching process in Zn–cyto c/a_5Ru^{III} below 100 K. At temperatures above 100 K, quenching did not follow simple Arrhenius behavior, but appeared to exhibit two distinct Arrhenius-type regions (within the temperature range of our measurements) with a transition temperature of ca. 150 K. Transient ODMR measurements at 1.2 K, a temperature at which spin–lattice relaxation between the sublevels of ^{3}ZnP* is effectively quenched, were carried out in order to test for spin selectivity in the triplet quenching process. The results, although affected by considerable experimental uncertainty because of the small quenching rates at low temperature, suggest that electron spin orientation is among the factors that influence the quenching rate in this type of system.

Experimental Section

Materials. The modified horse heart (Type VI) cytochrome *c* samples, Zn–cyto *c* and Zn–cyto c/a_5Ru^{III}, were generous gifts from Dr. J. R. Winkler, Brookhaven National Laboratory, New York. Their preparation is described in ref 18. These samples were purified further by chromatography on a cation exchange column (Watman, CM52). Reduced Zn–cyto c/a_5Ru^{II} was prepared by adding a molar excess of $Na_2S_2O_3$ to Zn–cyto c/a_5Ru^{III} under a N_2 atmosphere. The modified protein samples were stored in 100 mM potassium phosphate buffer at pH 7.0. For spectroscopic measurements at various temperatures, 50% glycerol (v/v) was added to each protein stock solution; the final protein concentration was ca. 8×10^{-5} M.

Phosphorescence Decay Kinetics. The sample was contained in a 2-mm-i.d. quartz tube that was placed in a slotted Cu block in thermal contact with a Cu disk attached to the end of a stainless steel tube. This assembly was inserted into a variable-temperature He flow cryostat (Janis Research Inc., Model DT). The temperature was measured by means of a calibrated Ge diode thermometer (Lake Shore Cryogenics, Inc., Model DRC 80) in thermal contact with the Cu disk. The sample temperature was controlled by regulating the flow of the cold He gas over the sample, as well as by two electrical heaters, one located immediately above the Cu disk and the other at the source of the refrigerant gas below the sample block. Variable-temperature measurements were made beginning at a high temperature and reducing the sample temperature because of the inefficiency of the heaters. Initially liquid N_2 was transferred into the outer reservoir of the cryostat, while the inner He reservoir was charged with He gas that was allowed to chill. Temperatures between room temperature and ca. 77 K were maintained within $\Delta T = \pm 1$ K for up to 10 min by controlling the He flow rate. To obtain temperatures below 77 K, liquid He was introduced into the inner reservoir and slowly bled into the sample chamber. Temperature control within ±1 K could be obtained between 10 and 77 K by means of the heaters. The phosphorescence spectrum was selected with a rotating can sector with a dead time of ca. 0.5 ms positioned in the optical plane of the Dewar. Phosphorescence decay kinetics were measured at 739 nm with a 0.67-m monochromator (McPherson, Inc., Model 788) set at 1.5-nm bandwidth. The sample was excited at 408 nm with a high-pressure Hg arc filtered through an aqueous IR filter and a 0.1-m grating monochromator (Instruments SA, Model H10) set at 16-nm bandwidth. Electronic shutters (Uniblitz, Inc., Model 26LOA3X5) with a 1-ms response time were placed in both excitation and emission paths in order to regulate the duration of excitation and emission. Phosphorescence decays, monitored over 5–6 lifetimes, were signal averaged and fit by computer to a single exponential by a Marquardt nonlinear least-squares algorithm. The intramolecular quenching rate constant for Zn–cyto c/a_5Ru^{III} was calculated from the relation $k_q = k_{app} - k_d$, where k_{app} is the phosphorescence decay constant of Zn–cyto c/a_5Ru^{III} and k_d is that of Zn–cyto *c* at the same temperature. Zn–cyto c/a_5Ru^{II} was not used as the control since it has been shown[18] that ^{3}ZnP* is quenched in this sample by electron transfer from Ru^{II}. In order to be certain that O_2 quenching was negligible in the temperature-dependence study, we performed control experiments on Zn–cyto *c* in which the sample was bubbled with Ar gas for 10 min before being transferred to the sample tube under a N_2 atmosphere. The decay kinetics were observed in the temperature range of interest and found to be indistinguishable from those of a sample that had not been deoxygenated.

Optically Detected Magnetic Resonance. The ODMR spectrometer has been described previously.[23,24] Measurements were made in zero magnetic field at ca. 1.2 K with the sample immersed in liquid He under reduced pressure. The ZFS of ^{3}ZnP* in the modified cytochrome *c* proteins were determined by ODMR slow-passage measurements, monitoring the phosphorescence maximum at 740 nm through the 0.67-m monochromator set for 3-nm band-pass. The results of several measurements at varying sweep rates were extrapolated to zero sweep rate to correct for transient effects. The individual sublevel decay constants at 1.2 K were measured with the microwave-induced delayed phosphorescence (MIDP)[25] and the microwave rapid-passage transient[26] methods. All ODMR measurements were signal averaged; the transient measurements were analyzed by computer with a nonlinear least-squares Marquardt algorithm as described above for the phosphorescence decay measurements.

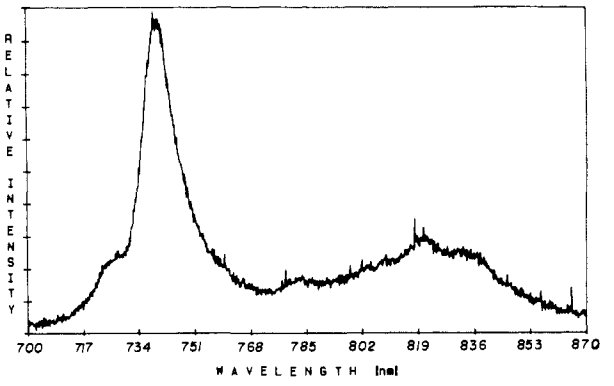

Figure 1. Phosphorescence spectrum (uncorrected) of Zn cytochrome *c* at 77 K. Excitation was at 408 nm with 16-nm band-pass, and the emission was collected with 3-nm monochromator bandwidth.

Results and Discussion.

Descriptive Background. A computer study based on the crystal structure of tuna cytochrome *c*[27] gives the distance of closest approach between His-33 and His-18 as 11.8 Å. The kinetics for the photoinduced electron transfer in the Zn–cyto c/a_5Ru^{III} protein is given in the following scheme:

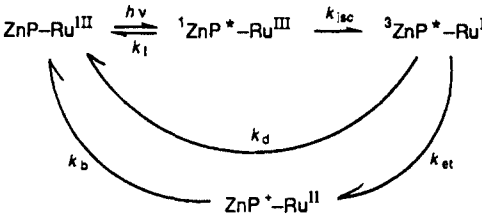

Recent measurements[18] have shown that the rate constant for the back-electron-transfer reaction (k_b) is about 1 order of magnitude greater than that of the forward reaction (k_{et}). We can monitor the electron-transfer process at various temperatures by direct measurement of the phosphorescence decay kinetics of ^{3}ZnP*. Since the redox potential for the $Ru(NH_3)_5(His)^{3+/2+}$ is 0.08 V, and those for Zn–cyto $c^{*+/*}$ and Zn–cyto $c^{*/*-}$ are −0.8 and 0.44 V, respectively[18], electron transfer can occur in both the Ru^{III} and Ru^{II} complexed Zn–cyto *c*. Hence, Zn–cyto *c*, rather than Zn–cyto c/a_5Ru^{II} was taken as the control molecule. The implicit assumption is that k_d in the scheme above is given at any temperature by the phosphorescence decay constant of ^{3}ZnP* observed in Zn–cyto *c*.

Temperature Dependence of the ^{3}ZnP* Phosphorescence. Phosphorescence from ^{3}ZnP* in either Zn–cyto *c* or Zn–cyto c/a_5Ru^{III} could not be detected at ambient temperature. Both samples gave indistinguishable phosphorescence spectra at reduced temperature, however; that of Zn–cyto *c* at 77 K is shown in Figure 1. Examples of the phosphorescence decays of both samples, along

(23) Ghosh, S.; Weers, J. G.; Petrin, M.; Maki, A. H. *Chem. Phys. Lett.* **1984**, *108*, 87.
(24) Zang, L. H. Ph.D. Thesis, University of California, Davis, 1988.
(25) Schmidt, J.; Veeman, W. S.; Van der Waals, J. H. *Chem. Phys. Lett.* **1969**, *4*, 341.
(26) Winscom, C. J.; Maki, A. H. *Chem. Phys. Lett.* **1971**, *12*, 264.
(27) Mayo, S. L.; Ellis, W. R., Jr.; Crutchley, R. J.; Gray, H. B. *Science* **1986**, *233*, 948.

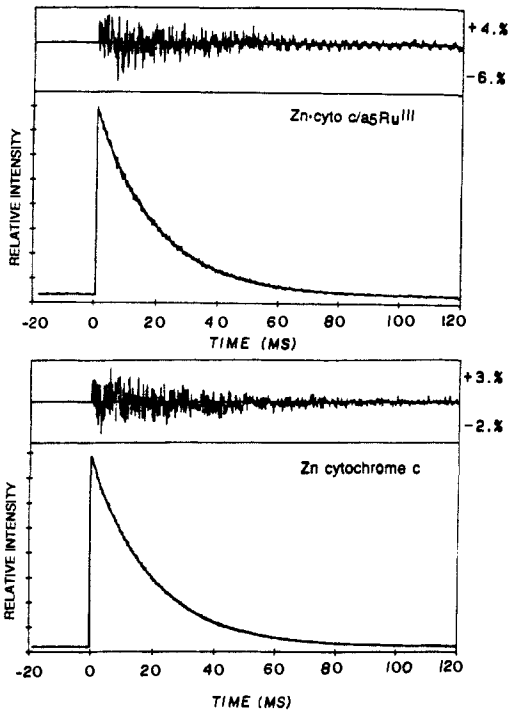

Figure 2. Phosphorescence decays of Zn cytochrome *c* and its Ru^{III} derivative at 77 K. The residuals for a single exponential fitting of the decays are shown. Samples were excited for 160 ms.

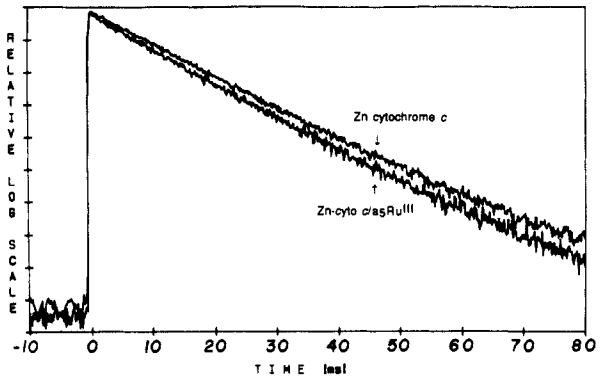

Figure 3. Semilogarithmic plots of the decay data presented in Figure 2. The small difference in decay lifetime is clearly resolved.

with the residuals from single exponential fits of the data are shown in Figure 2. Semilogarithmic plots of these data, which are compared in Figure 3, show that the decay constants clearly differ from each other. The first-order decay constants of Zn–cyto *c* and of Zn–cyto c/a_5Ru^{III} are plotted vs temperature in Figure 4. The decay constant of Zn–cyto *c* is found to be temperature independent over the entire range of measurement, 15–200 K, while that of Zn–cyto c/a_5Ru^{III} is temperature independent up to ca. 100 K, but increases significantly above this temperature. For the Ru^{III}-derivatized protein, the phosphorescence decay first becomes measureable at ca. 170 K, where $k_{app} \sim 175\ s^{-1}$. The analysis of 19 independent phosphorescence decays of Zn–cyto *c* between 15 and 200 K yielded $k_d = 47.5 \pm 0.13\ s^{-1}$. A similar analysis of 15 phosphorescence decays of Zn–cyto c/a_5Ru^{III} in the temperature-independent range, 11–91 K, gave $k_{app} = 51.1 \pm 0.18\ s^{-1}$. The uncertainties indicated are the estimated standard deviations of the means of the measured rate constants.[28] From these measurements we obtain $k_q = 3.6 \pm 0.22\ s^{-1}$ in the temperature-independent region below 100 K. Possible origins of this small temperature-independent k_q will be discussed below. The results of all measurements are given in Figure 5, where ln k_q is

(28) Bevington, P. R. *Data Reduction and Error Analysis for the Physical Sciences*; McGraw-Hill: New York, 1969.

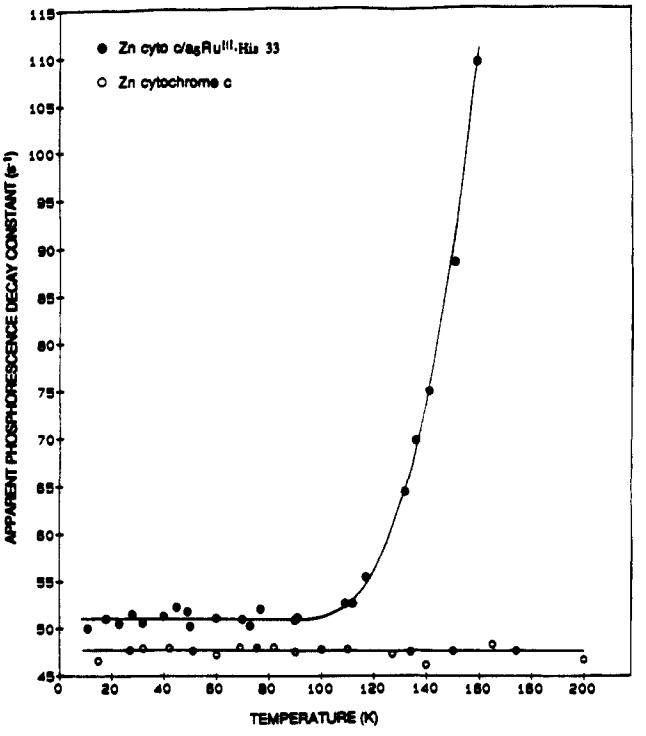

Figure 4. Plot of the phosphorescence decay constants of Zn–cyto *c* (○), and Zn–cyto c/a_5Ru^{III} (●) vs temperature.

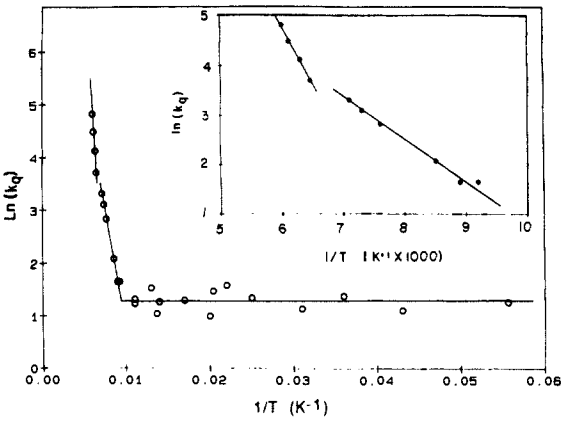

Figure 5. Plot of the logarithm of the quenching rate constant of Zn–cyto c/a_5Ru^{III} vs $1/T$. The two nonzero slopes are 1.6 and 5.6 kcal/mol.

plotted vs T^{-1}. Above 100 K, the quenching rate constant becomes temperature dependent, indicating the coupling of electron transfer to thermal vibrations and fluctuations.[22] The inset of Figure 5 shows clearly that the thermally activated electron-transfer range above 100 K does not exhibit a simple Arrhenius behavior. Rather, the data can be fit to two Arrhenius regions having a discontinuity at ca. 150 K. The slopes in these two regions give apparent activation energies of 1.6 and 5.6 kcal/mol, below and above the transition-temperature region, respectively. If the data points above 150 K are extrapolated to 298 K, a value of $k_q \cong 2 \times 10^5\ s^{-1}$ is obtained, which is in line with the results ($k_q = 7.7 \times 10^5\ s^{-1}$) of transient absorption measurements at room temperature.[18] The fitting of these data in the 100–200 K region to two Arrhenius-type regions may be an oversimplification, and measurements over a larger temperature range could yield a more complicated behavior. Attempts to fit our data above 100 K with either a semiclassical[19] or a quantum mechanical[21] expression employing a single vibrational mode produced very poor agreement. Thus, we find that thermally activated electron transfer undergoes a considerable increase in the apparent activation energy with a transition temperature of ca. 150 K. This temperature is well below the glassing temperature of the aqueous glycerol medium (ca. 240 K) and, thus, suggests changes in internal protein

Table I. Zero-Field Splittings and ODMR LinesWidths of Cytochrome *c* Derivatives

sample	ν_1 ($\Delta\nu_1$)[a]	ν_2 ($\Delta\nu_2$)[a]	$\lvert D\rvert$[a]	$\lvert E\rvert$[a]
Zn–cyto *c*	0.812 (36)	1.255 (41)	1.034	0.221
Zn–cyto *c*/a_5Ru^{II}	0.816 (35)	1.256 (39)	1.036	0.220
Zn–cyclo *c*/a_5Ru^{III}	0.817 (50)	1.253 (55)	1.035	0.218

[a] All frequencies are given in gigahertz, except for $\Delta\nu$, which is the full width of the ODMR line at half-maximum intensity in megahertz. The phosphorescence is monitored at 739.5 nm with 3-nm bandwidth. Transition frequencies are extrapolated to zero sweep rate to eliminate rapid-passage effects.

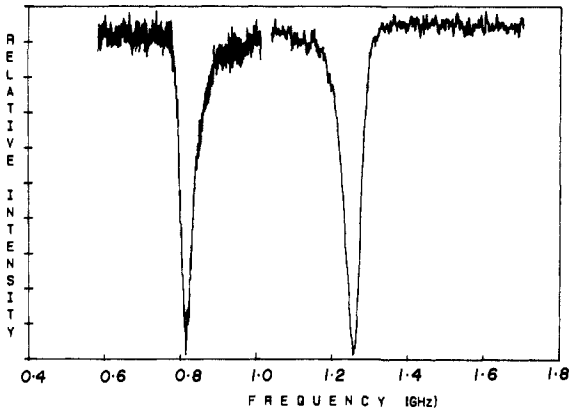

Figure 6. ODMR slow-passage $|D| - |E|$ (lower frequency) and $|D| + |E|$ (higher frequency) signals of Zn cytochrome *c* at 1.2 K. Sweep rates were 25 and 250 MHz/s, respectively. Signal averaging was carried out for 134 and 149 scans, respectively. Phosphorescence was monitored at 740 nm with 3-nm bandwidth.

dynamics and/or structure that set in at this temperature. Similar inflections in thermally activated electron transport occur in a large number of photosystems at ca. 150 K; they have been attributed[29] to the freezing out of specific protein fluctuations below this temperature. The low-temperature rate constant obtained in this work is in accord with our measurements of Zn/Ru-modified myoglobins,[24] although it is somewhat less than that found previously by Hoffman and co-workers[9] in Zn/Fe hybrid hemoglobins (9 ± 4 s^{-1}) in which the distance between the redox centers is larger.

Optically Detected Magnetic Resonance. The results of the slow-passage ODMR measurements in which the $|D| + |E|$ and the $|D| - |E|$ transitions were measured are given in Table I. The ODMR signals of Zn–cyto *c* are shown in Figure 6. The ZFS are the same within experimental error (±5 MHz) for Zn–cyto *c* and the Ru^{II} and Ru^{III} derivatives, indicating that the presence of Ru in either oxidation state has little effect on the average local environment of the porphyrin. The ODMR line widths, however, are significantly larger for Zn–cyto *c*/a_5Ru^{III} than they are for the other derivatized proteins. The greater line width arises from increased heterogeneity in the local protein/solvent environment. Since the ODMR measurements are made at 1.2 K where electron transfer would be controlled by nuclear tunneling,[30] it is possible that the heterogeneity of the environment contains a measureable contribution from atoms that have been displaced from their normal positions by tunneling events. This explanation would support electron-transfer contributions to triplet state quenching below 100 K. On the other hand, the broadening could be due, as well, to greater static heterogeneity in Zn–cyto *c*/a_5Ru^{III}.

Triplet Sublevel Kinetics. Since the measurement of individual triplet state sublevel kinetics by ODMR are made at 1.2 K, and the sample is chilled rapidly to this temperature, it was essential to determine whether the decay kinetics were sensitive to the cooling rate of the sample. Thus, we measured k_{app} for the Ru-derivatized samples and k_d for Zn–cyto *c* in samples that had been cooled rapidly to 77 K by immersion in liquid N_2. The results

(29) Hales, B. J. *Biophys. J.* **1976**, *16*, 471.
(30) DeVault, D.; Chance, B. *Biophys. J.* **1966**, *6*, 825.

Table II. Triplet Sublevel Decay Constants and Relative Radiative Rate Constants of Cytochrome *c* Derivatives Obtained from Microwave-Induced Phosphorescence Transients

	k_x (s^{-1})[a]	k_y (s^{-1})[b]	k_z (s^{-1})[b]	κ (s^{-1})[c]	$k_{x,r}$[d]	$k_{y,r}$[d]	$k_{z,r}$[d]
Zn–cyto *c*	31.3	92.6	21.3	48.4	0.04	1.0	0.37
Zn–cyto *c*/a_5Ru^{II}	31.5	93.9	22.5	49.3	0.09	1.0	0.37
Zn–cyto *c*/a_5Ru^{III}	35.4	98.9	22.0	52.1	0.09	1.0	0.38

[a] Calculated from data in next three columns. See text. [b] Obtained from analysis of the $|D| - |E|$ phosphorescence transient. [c] κ is the observed phosphorescence decay constant at 77 K for a rapidly chilled sample. It is referred to in the text as k_d for Zn–cyto *c* and k_{app} for Zn–cyto *c*/$a_5Ru^{II,III}$. [d] Relative values obtained from analysis of $|D| - |E|$ and $|D| + |E|$ phosphorescence transients. See text.

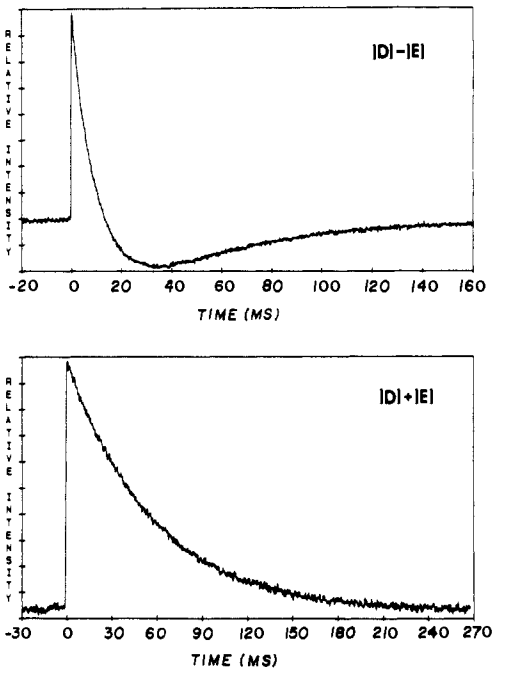

Figure 7. Microwave-induced rapid-passage transients of Zn–cyto *c* at 1.2 K. Microwave sweep rate was 760 GHz/s for each transition. The $|D| + |E|$ signal polarity was inverted in the figure. The transient response is actually negative.

are presented in Table II. Both k_{app} and k_d were found to be ca. 1 s^{-1} larger at 77 K in the rapidly chilled samples than in the gradually cooled samples. However, $k_q = k_{app} - k_d$ was found to be 3.7 s^{-1}, in excellent agreement with the low-temperature limiting value obtained for the gradually cooled samples. The small increase in decay constants for the rapidly cooled samples, which may be significant, is apparently an intrinsic property of the porphyrin triplet state of the protein and is not related to the quenching mechanism. It is interesting that $k_{app} - k_d = 0.9 \pm 0.9$ s^{-1} for Zn–cyto *c*/a_5Ru^{II} at 77 K may represent a barely detectable quenching process.

(a) Microwave-Induced Phosphorescence Transients. Microwave rapid-passage transient measurements[27] were carried out on each sample at 1.2 K. Examples of the phosphorescence responses for the $|D| - |E|$ and $|D| + |E|$ transitions of Zn–cyto *c* are shown in Figure 7. The clearly exhibited biexponential nature of the $|D| - |E|$ response indicates that both triplet-state sublevels connected by this transition have radiative character. We define the sublevels connected by the $|D| - |E|$ transition as T_y and T_z. T_z is the sublevel common to both the $|D| \pm |E|$ transitions. Computer analysis of the $|D| + |E|$ transient reveals that it is similarly biexponential, consisting of a major component with a negative preexponential factor and a minor somewhat shorter lived component with positive preexponential factor. The major component has the same decay constant as the longer lived component of the $|D| - |E|$ response and is accordingly assigned to the decay of the T_z sublevel. The minor decay component,

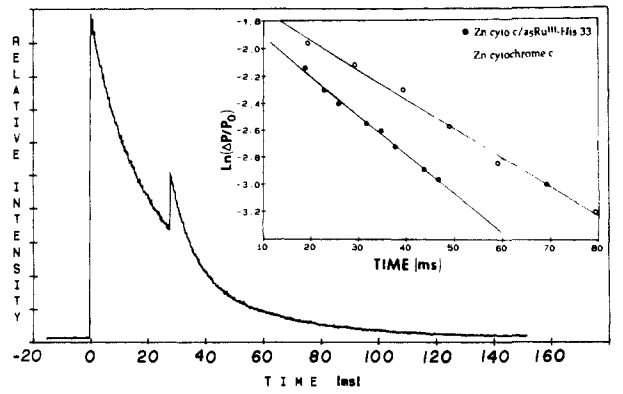

Figure 8. Typical $|D| - |E|$ MIDP signal of Zn–cyto *c*. The inset shows a plot of the logarithm of the normalized MIDP response vs *t* for Zn–cyto *c* and Zn–cyto c/a_5Ru^{III}. The slope gives the first-order decay constant of the T_z sublevel in the respective protein.

assigned to T_x, could not be determined accurately because of its vanishingly small radiative strength. The value of k_x was obtained from the relation, $3\kappa = k_x + k_y + k_z$, where κ is the average ^{3}ZnP decay constant observed under conditions of rapid spin–lattice relaxation, i.e., at 77 K. The temperature-dependent decay data presented earlier reveal no measureable variation in κ between 10 and 77 K, so the use of the 77 K data to obtain k_x is justified. The values of k_y and k_z obtained from analysis of the $|D| - |E|$ transient response are given in Table II along with k_x, obtained as described above. The values of k_z obtained from the $|D| + |E|$ transient analysis are in good agreement with the values reported in Table II. The relative sublevel radiative rate constants, which are proportional to the preexponential factors in the computer analysis of the microwave-induced phosphorescence transients, are included in Table II.

(b) Microwave-Induced Delayed Phosphorescence. Sublevel decay constants obtained from microwave-induced phosphorescence transient measurements may be subject to error if they are not corrected for the optical pumping effect by extrapolation to zero incident light intensity. The data presented in Table II were not corrected for this effect, but they are in good agreement with rate constants obtained from MIDP measurements that are not subject to this source of error, and which we discuss next. In the MIDP experiment, a microwave pulse is applied during the decay of the phosphorescence in the absence of optical pumping. A typical MIDP response of Zn–cyto *c* to a microwave pulse applied at the $|D| - |E|$ frequency is shown in Figure 8. The height of the phosphorescence "echo" is proportional to the population difference between the T_z and T_y sublevels. For sufficiently long delay times, the T_y population is negligible; a semilogarithmic plot of the echo height vs time is linear and represents the first-order decay of the population of T_z. These plots are shown in the insert of Figure 8 for Zn–cyto *c* and for Zn–cyto c/a_5Ru^{III}. The decay constant, k_z, of the Ru^{III} derivative is clearly greater than that of Zn–cyto *c*; the difference is attributed to quenching *of the T_z sublevel*. Accurate values of k_y and k_z were obtained by analyzing the transient responses themselves with a two-component fit. Attempts to obtain MIDP responses from a pulse applied at the $2|E|$ frequency were unsuccessful, probably because of the small steady-state populations of both T_x and T_y. MIDP measurements were attempted with the $|D| + |E|$ microwave frequency. An analogous two-component analysis of the transient response did not produce accurate values of k_x since T_x contributes less than 10% to the transient because of its weak radiative strength (Table II), although reliable values of k_z were obtained. Also, the normal MIDP analysis (Figure 8) could not be applied to this transition since T_z and T_x decay with comparable lifetimes. The values of the sublevel decay constants obtained from the MIDP measurements are given in Table III. The value of k_x was calculated from κ, as described in the previous section.

Sublevel-Selective Quenching. Because of the isolation of the ^{3}ZnP electron donor sublevels that occurs at pumped He temperature, it is possible, in principle, to measure the quenching rate

Table III. Triplet Sublevel Decay Constants and Quenching Rate Constants at 1.2 K Obtained from Microwave-Induced Delayed Phosphorescence Measurements

	k_x (s^{-1})[a]	k_y (s^{-1})[b]	k_z (s^{-1})[c]	$k_{x,q}$ (s^{-1})[d]	$k_{y,q}$ (s^{-1})[d]	$k_{z,q}$ (s^{-1})[d]
Zn–cyto *c*	32.0	92.0	21.2			
Zn–cyto c/a_5Ru^{II}	33.3	92.1	22.5	1.3	0.1	1.3
Zn–cyto c/a_5Ru^{III}	32.1	97.8	26.4	0.1	5.8	5.2

[a] Calculated from κ and data in the next two columns. See text. [b] From MIDP measurements of $|D| - |E|$ transition. [c] Obtained by averaging MIDP measurements of $|D| - |E|$ and $|D| + |E|$ transitions. See text. [d] Calculated from $k_i - k_j$ (Zn–cyto *c*).

constants of the individual sublevels. This was, in fact, the primary goal of this research. The ^{3}ZnP sublevels differ in the orientation of the $S = 1$ spin angular momentum in the ZnP molecular framework. The *z*-axis is normal to the porphyrin plane,[31] while the in-plane *x*- and *y*-axes have not been located in Zn–cyto *c*. The spin angular momentum of the T_i sublevel is oriented in the plane normal to the *i*-axis. Thus, the spin angular momentum of T_z is confined to the porphyrin plane. If quenching is due to electron transfer, any electron spin dependence of quenching should be reflected in the electronic matrix element, H_{RP}, of the Marcus theory.

$$k_{et} = (2\pi/\hbar)\,|H_{RP}|^2 F \qquad (1)$$

In eq 1, *F* is a thermally averaged Franck–Condon factor. The nuclear motion has been treated by classical[32] and semiclassical[33] means and by a quantum mechanical model.[34] In the low-temperature regime in which ODMR is possible, *F* reduces to a nuclear tunneling term. Nuclear tunneling should severely limit electron transfer over distances as large as that found in Zn–cyto $c/a_5Ru^{II,III}$. The rate constants for quenching in the temperature-independent range are the order of 10% or less of the phosphorescence decay constants, making them very difficult to measure. We believe that the most reliable individual sublevel kinetic data appear in Table III, having been measured by the MIDP method. Can any conclusions about spin–sublevel selectivity of the quenching process be drawn from these data? Sublevel selectivity would be manifested by any $k_{i,q}$ that deviates significantly from the average rate constant for the triplet state, $k_q = 3.6 \pm 0.22\ s^{-1}$. The most reliable individual rate constant in this table is $k_{z,q}$, which has an estimated uncertainty of $\pm 1.4\ s^{-1}$. Although $k_{z,q}$ and k_q differ by only about their combined uncertainties, we can conclude with moderate confidence that the T_z sublevel embodies a greater than average probability for quenching by Ru^{III}. It might appear that the quenching rate constant of T_y also exceeds k_q, but the greater estimated uncertainty of $k_{y,q}$ ($\pm 2.5\ s^{-1}$) gives relatively little confidence in this conclusion. Finally, because of the indirect method by which the decay constants of T_x had to be obtained, no conclusions can be reached about the quenching of this sublevel. Regarding individual sublevel electron transfer in Zn–cyto c/a_5Ru^{II}, the smaller values obtained for $k_{y,q}$, and $k_{z,q}$ from the MIDP measurements are in accord with the lower average k_q measured at 77 K; the uncertainties, however, are such that no conclusions can be reached about sublevel selective quenching of ^{3}ZnP* by Ru^{II}.

Temperature-Independent Quenching. Although the thermally activated quenching of ^{3}ZnP* above 100 K results from electron transfer to Ru^{III},[18] the origin of the inefficient, temperature-independent quenching below 100 K may have several origins. The possibility of nuclear-tunneling-assisted electron transfer has already been mentioned. Whether or not electron transfer is the

(31) Van Dorp, W. G.; Soma, M.; Kooter, J. H.; Van der Waals, J. H. *Mol. Phys.* **1974**, *28*, 1551.
(32) Marcus, R. A. In *Tunneling in Biological Systems*; Chance, B., et al., Eds.; Academic: New York, 1979; p 109.
(33) Hopfield, J. J. *Proc. Natl. Acad. Sci. U.S.A.* **1974**, *71*, 3644.
(34) Jortner, J. *J. Chem. Phys.* **1976**, *64*, 4860; *J. Am. Chem. Soc.* **1980**, *102*, 6676.

appropriate mechanism, the inefficiency of this low-temperature quenching process points to the negligible contribution of tunneling to electron transfer in Zn-cyto $c/a_5Ru^{II,III}$. Other possible mechanisms are magnetic dipole induced relaxation by the magnetic moment of Ru^{III} and energy transfer. The energy transfer process would require the existence of a suitable acceptor energy level of a_5Ru^{III}his below that of $^3ZnP^*$ (39 kcal/mol). Since $10Dq$ for $Ru^{III}(NH_3)_6$ has been estimated to be ca. 91 kcal/mol,[35] $t_2 \rightarrow e$ excitations would not be effective. On the other hand, the degeneracy of the t_2^5 configuration is reduced by the combination of an axial ligand field distortion and spin-orbit coupling to produce some low-lying electronic states[35] that could conceivably quench $^3ZnP^*$ by an energy transfer mechanism.

Transitions to these states should be highly forbidden by electric dipole selection rules, and thus coupling to the $^3ZnP^*$ might be expected to occur preferentially either by an electronic exchange mechanism[36] or by a magnetic dipolar mechanism. The latter mechanism should be sensitive to the spin orientation of the donor sublevel of $^3ZnP^*$, but we do not know enough about the electronic energy level structure of a_5Ru^{III}his to speculate further.

Thermally Activated Electron Transfer. With regard to the thermally activated electron transfer occurring above 100 K, the appearance of two distinct Arrhenius-type regions with differing activation energies is of interest. This particular temperature dependence may be an oversimplification because of the limited temperature range investigated. However, simple Arrhenius behavior definitely is not the case. The observed temperature dependence could be the result of conformationally gated electron transfer proposed recently by Hoffman and Ratner,[6] which has received experimental support from McLendon, et al.[7] Conformational gating is based on a theory of Agmon and Hopfield,[37] in which reaction rates in proteins are modulated by diffusional motions of the medium perpendicular to the reaction coordinate. The protein medium assumes the role of the outer solvent sphere in the Marcus-Hush theory,[20] while the inner solvent sphere coordinates (local bond lengths and angles) undergo Hamiltonian or "ballistic" motion.[37] Hoffman and Ratner show that in a protein such as cytochrome c, which undergoes a structural change upon reduction,[38] electron transfer can be conformationally gated if two or more stable protein conformations exhibit differing rate constants for electron transfer. It is expected that there will be a change in the activation energy for electron transfer as the protein motions slow down and the medium becomes frozen into a single stable conformation, i.e., that which is energetically most favorable to the precursor state. Other, less specific models for protein dynamics could also lead to non-Arrhenius behavior, however.

(35) Sham, T. K. *J. Am. Chem. Soc.* **1983**, *105*, 2269.
(36) Dexter, D. L. *J. Chem. Phys.* **1953**, *21*, 836.
(37) Agmon, N.; Hopfield, J. J. *J. Chem. Phys.* **1983**, *78*, 6947; *Ibid.* **1983**, *79*, 2042.

Conclusions

Measurements of the rate constant for the decay of ^3ZnP in Zn-cyto c/a_5Ru^{III} over a wide range of temperature reveal a temperature-independent region below 100 K for quenching of ^3ZnP by Ru^{III}, with a rate constant of $k_q = 3.6 \pm 0.22\ s^{-1}$. In this range, electron transfer, which is coupled to nuclear tunneling, may be responsible for the quenching. Other possible mechanisms that are discussed are energy transfer and magnetic-dipole-induced quenching. Above 100 K, two regions of Arrhenius-type activated electron transfer are found with $E_a = 1.6$ kcal/mol below 150 K and $E_a = 5.6$ kcal/mol above this transition temperature. It is suggested that this behavior may be a manifestation of conformational gating utilizing two or more stable protein conformations. Transient ODMR measurements made at 1.2 K, where spin-lattice relaxation is quenched suggest that the T_z sublevel of ^3ZnP has a quenching rate constant ($k_{z,q} = 5.2 \pm 1.4\ s^{-1}$) that exceeds the average of the three sublevels, and thus that the process, which governs the temperature-independent quenching of ^3ZnP by Ru^{III}, varies with the orientation of spin angular momentum in the precursor state. The larger ODMR line widths exhibited by Zn-cyto c/a_5Ru^{III} relative to Zn-cyto c and Zn-cyto c/a_5Ru^{II} result from greater local heterogeneity of the porphyrin environment in the former protein. The increased local heterogeneity may result from disorder induced by tunneling processes, or the disordering may be static.

Acknowledgment. We are grateful to J. R. Winkler for a gift of the proteins used in these measurements and for several informative discussions. This research was partially supported by a research grant (CHE 85-08752) from the National Science Foundation and a Graduate Student Research Award to L.-H.Z. from the University of California, Davis.

(38) Takano, T.; Richardson, R. E. *J. Mol. Biol.* **1981**, *153*, 79, 95.

Synthesis of Cytochalasins: The Route to Sulfur-Bridged [11]Cytochalasans

E. Vedejs,* J. G. Reid, J. D. Rodgers, and S. J. Wittenberger

Contribution from the Chemistry Department, University of Wisconsin, Madison, Wisconsin 53706. *Received September 7, 1989*

Abstract: The sulfur-mediated syntheses of the sulfur-bridged [11]cytochalasans **23** and **30** are described in full. Key steps include the highly selective Diels-Alder addition of **5a** and **6** to give **7a**, the generation and hetero-Diels-Alder trapping of the transient thioaldehyde **13**, and the conversion of **19** into the sulfur-bridged 11-membered carbocycles **23** + **24** via a 2,3-sigmatropic rearrangement of an intermediate sulfonium ylide **22**. Treatment of **23** with LDA followed by methyl iodide gave **30** via a bridgehead enolate **29**. Structure **30** contains all of the ring carbon atoms and all but two of the asymmetric centers found in the most complex of the naturally occurring cytochalasins and zygosporins.

The cytochalasins have been known since the isolation and structure determination of cytochalasin B (phomin, **1**) by Rothweiler and Tamm (1966) and independently by Turner et al. (1967).[1,2] Several related 11-membered carbocycles ("[11]-cytochalasans") were soon discovered including zygosporins A (later renamed cytochalasin D, **2**) and E (**3**).[3,4] The lactam ring common to these substances is derived from phenylalanine, but closely related structures that incorporate tryptophan (chaeto-

(1) Rothweiler, W.; Tamm, C. *Experientia* **1966**, *22*, 750.
(2) Aldridge, D. C.; Armstrong, J. J.; Speake, R. N.; Turner, W. B. *Chem. Commun.* **1967**, 26.
(3) Hayakawa, S.; Matsushima, T.; Kimura, T.; Minato, H.; Katagiri, K. *J. Antibiot. (Tokyo)* **1968**, *21*, 523.
(4) Aldridge, D. C.; Turner, W. B. *J. Chem. Soc. C* **1969**, 923. Minato, H.; Katayama, T. *J. Chem. Soc. C* **1970**, 45. Aldridge, D. C.; Burrows, B. F.; Turner, W. B. *Chem. Commun.* **1972**, 148.

0002-7863/90/1512-4351$02.50/0